Decay of a charged scalar and Dirac fields in the Kerr-Newman-de Sitter background

R. A. Konoplya* and A. Zhidenko†

Instituto de Física, Universidade de São Paulo, C.P. 66318, 05315-970, São Paulo-SP, Brazil

(Received 18 July 2007; published 17 October 2007)

We find the quasinormal modes of the charged scalar and Dirac fields in the background of the rotating charged black holes, described by the Kerr-Newman-de Sitter solution. The dependence of the quasinormal spectrum upon the black hole parameters mass M, angular momentum a, charge Q, as well as on values of the Λ-term and a field charge q is investigated. Special attention is given to the near extremal limit of the black hole charge. In particular, we find that for both scalar and Dirac fields, charged perturbations decay quicker for $q > 0$ and slower for $q < 0$ for values of black holes charge Q less than some threshold value, which is close to the extremal value of charge and depend on parameters of the black holes.

DOI: 10.1103/PhysRevD.76.084018 PACS numbers: 04.30.Nk, 04.50.+h

I. INTRODUCTION

The quasinormal (QN) spectrum of black holes has been extensively investigated during recent years for a great variety of black hole backgrounds and fields, because it is an important characteristic for observation of the gravitational waves [1], stability analysis [2], and AdS/CFT calculations of temperature Green functions [3]. Special attention has been paid to perturbations of a scalar field [4], as a simplest model, when the influence of the spin of the field is neglected. When one considers the charged black hole, the scalar electrodynamic can successfully model the interaction of the charged field with the electromagnetic background of the black hole. Therefore the calculation of the quasinormal modes (QNMs) of charged fields, initiated in [5] for the charged scalar field in the Reissner-Nordstöm and dilaton backgrounds, was continued in further research [6–9]. In particular, in [7] the quasinormal modes of the massive charged scalar field were found with the WKB accuracy. In [5,7] it was shown that the quasinormal modes, corresponding to the charged scalar field, decay quicker than those of the neutral field unless the black hole charge is larger than some large near extremal value. This is opposite to the behavior at asymptotically late times, characterized by the so-called "tail" decay, when the charged scalar field decays slower, and therefore, dominates at asymptotically late times [10]. Yet, the quasinormal frequencies calculated for Reissner-Nordström black holes in [5–7] with the help of the WKB method need better accuracy and cannot be trusted near the extremal limit, especially for the scalar case, because the effective potential is frequency dependent in this case, and the WKB equation for the QN frequency must be solved together with a frequency dependent equation determining the position of the maximum of the effective potential.

On the other hand, one has a much richer physical situation, when one takes into consideration all the relevant parameters, such as black hole angular momentum and the cosmological term, i.e. when one starts from the Kerr-Newman-de Sitter (KNdS) black hole as a gravitational background. In this paper we achieve both the above mentioned aims: to find QN modes with very high accuracy, by using the convergent Frobenius expansion, and to consider the most general relevant black hole solution of the general relativity, KNdS solution. The latter gives us dependence of the QN spectrum on a great number of parameters: charge of the black hole Q, charge of the field q, normalized angular momentum of the black hole a, the cosmological term Λ.

The paper is organized as follows: Sec. II gives some basic formulas on the KNdS metric and on radial wave equation for charged massless scalar and Dirac fields, and also discusses the system of units we used for showing the QNMs. Section III reviews the obtained numerical results. In the conclusion we summarize the obtained results.

II. BASIC FORMULAS

In the Boyer-Lindquist coordinates the Kerr-Newman-de Sitter metric has the form [11]

$$ds^2 = -\rho^2\left(\frac{dr^2}{\Delta_r} + \frac{d\theta^2}{\Delta_\theta}\right) - \frac{\Delta_\theta \sin^2\theta}{(1+\alpha)^2\rho^2}[adt - (r^2 + a^2)d\varphi]^2 + \frac{\Delta_r}{(1+\alpha)^2\rho^2}(dt - a\sin^2\theta d\varphi)^2, \quad (1)$$

where

$$\Delta_r = (r^2 + a^2)(1 - \alpha r^2/a^2) - 2Mr + Q^2,$$
$$\alpha = \Lambda a^2/3, \qquad \Delta_\theta = 1 + \alpha\cos^2\theta, \quad (2)$$
$$\rho^2 = r^2 + a^2\cos^2\theta.$$

The electromagnetic background of the black hole is given by the four-vector potential

$$A_\mu dx^\mu = -\frac{Qr}{(1+\alpha)^2\rho^2}(dt - a\sin^2\theta d\varphi). \quad (3)$$

*konoplya@fma.if.usp.br
†zhidenko@fma.if.usp.br

The charged scalar and Dirac fields in curved space-time are described by the following equations of motion:

$$\Phi^{(0)}_{;\mu\nu}g^{\mu\nu} - iqA_\mu g^{\mu\nu}(2\Phi^{(0)}_{;\nu} - iqA_\nu\Phi^{(0)}) - iqA_{\mu;\nu}g^{\mu\nu}\Phi^{(0)} = 0, \qquad \text{(charged scalar)} \quad (4)$$

$$\gamma^a e^\mu_a(\partial_\mu + \Gamma_\mu + qA_\mu)\Phi^{(1/2)} = 0, \qquad \text{(charged Dirac)} \quad (5)$$

where q is the charge of particles and A_a is the electromagnetic potential of the background.

Some manipulation with scalar and Dirac equations allow in some separable form (see [11] and references therein). The existence of the Killing vectors ∂_t, ∂_ϕ, implies the exponential harmonics of the following form $\sim e^{-i\omega t}$, $\sim e^{im\phi}$). After the separation of the angular, radial, and time variables

$$\Phi^{(s)}(t, r, \theta, \phi) \propto e^{-i\omega t}e^{im\phi}S(\theta)R(r),$$

one can obtain the equation for the angular part [11]

$$\left\{\frac{d}{dx}(1+\alpha x^2)(1-x^2)\frac{d}{dx} + \lambda - s(1-\alpha) + \frac{(1+\alpha)^2}{\alpha}\xi^2 - 2\alpha x^2 - \frac{(1+\alpha)^2m^2}{(1+\alpha x^2)(1-x^2)} - \frac{(1+\alpha)(s^2+2smx)}{1-x^2} + \frac{1+\alpha}{1+\alpha x^2}\left[2s(\alpha m - (1+\alpha)\xi)x - \frac{(1+\alpha)^2}{\alpha}\xi^2 - 2m(1+\alpha)\xi + s^2\right]\right\}S_s(x) = 0, \quad (6)$$

where s is the spin of the field ($s = 0, 1/2$ for the scalar and Dirac field, respectively), $x = \cos\theta$, $\xi = a\omega$, and λ is the separation constant (for the nonrotating case $\lambda = \ell(\ell+1) - s(s-1)$, where $\ell \geq s$ is the positive (half)integer multipole number). The angular equation can be solved numerically with respect to λ for each value of ω by using the three-term recurrence relation [11].

The equation for the radial part is

$$\left\{\Delta_r^{-s}\frac{d}{dr}\Delta_r^{s+1}\frac{d}{dr} + \frac{1}{\Delta_r}\left(K^2 - isK\frac{d\Delta_r}{dr}\right) + 4is(1+\alpha)\omega r - \frac{2\alpha}{a^2}(s+1)(2s+1)r^2 + 2s(1-\alpha) - 2isqQ - \lambda\right\}R_s(r) = 0, \quad (7)$$

where $K = [\omega(r^2 + a^2) - am](1+\alpha) - qQr$.

Generally, this equation has five regular singularities: the event horizon r_+, the internal horizon r_-, the cosmological horizon r'_+, the spatial infinity, and one more singularity at r'_-. One should note that $r_\pm$ and $r'_\pm$ are roots of equation $\Delta_r = 0$.

In the limit of $\Lambda \to 0$ one has

$$r_\pm \to M \pm \sqrt{M^2 - a^2 - Q^2}, \qquad r'_\pm \to \pm\frac{a}{\sqrt{\alpha}},$$

and, therefore, the spacial infinity becomes an irregular singularity [11].

By the definition, the QNMs are eigenfrequencies ω of (7) which satisfy the following boundary conditions (b.c.): ψ represents purely ingoing waves at the event $r = r_+$ horizon and purely outgoing waves at the cosmological horizon $r = r'_+$ (or the spacial infinity if $\Lambda = 0$).

Now we introduce the new function, which is regular at these two points if the QNM b.c. are satisfied

$$y(r) = r^{2s+1}\left(\frac{r - r_+}{r - r_-}\right)^{s+2iK(r_+)/\Delta'_r(r_+)}e^{-iB(r)}R(r), \quad (8)$$

where $\frac{dB(r)}{dr} = \frac{K}{\Delta_r}$.

The appropriate Frobenius series is

$$y(r) = \sum_{n=0}^{\infty} a_n\left(\frac{r - r_+}{r - r_-}\right)^n\left(\frac{1 - \rho r_-/r_+}{1 - \rho}\right)^n, \quad (9)$$

where $\rho = r_+/r'_+$.

Substituting (8) and (9) into (7), one can obtain the N-term recurrence relation for the coefficients a_i

$$\sum_{j=0}^{\min(N-1,i)} c^{(N)}_{j,i}(\omega)a_{i-j} = 0, \quad \text{for } i > 0, \quad (10)$$

where N depends on the black hole parameters. For the particular Schwarzschild case $N = 3$, but for the general case under consideration N is higher than 3. We decrease the number of terms in the recurrence relation using the *Gaussian eliminations*:

$$c^{(k)}_{j,i}(\omega) = c^{(k+1)}_{j,i}(\omega), \quad \text{for } j = 0, \quad \text{or } i < k,$$

$$c^{(k)}_{j,i}(\omega) = c^{(k+1)}_{j,i}(\omega) - \frac{c^{(k+1)}_{k,i}(\omega)c^{(k)}_{j-1,i-1}(\omega)}{c^{(k)}_{k-1,i-1}(\omega)}.$$

After one finds $c^{(3)}_{j,i}$ numerically, he can solve the equation with *infinite continued fraction* (see [12] for more details)

$$c^{(3)}_{1,n+1} - \frac{c^{(3)}_{2,n}c^{(3)}_{0,n-1}}{c^{(3)}_{1,n-1}-}\,\frac{c^{(3)}_{2,n-1}c^{(3)}_{0,n-2}}{c^{(3)}_{1,n-2}-}\cdots\frac{c^{(3)}_{2,2}c^{(3)}_{0,1}}{c^{(3)}_{1,1}} = \frac{c^{(3)}_{0,n+1}c^{(3)}_{2,n+2}}{c^{(3)}_{1,n+2}-}\,\frac{c^{(3)}_{0,n+2}c^{(3)}_{2,n+3}}{c^{(3)}_{1,n+3}-}\cdots \quad (11)$$

Since we can find the separation constant λ for each particular value of ω, (11) allows to find QNMs with the desired precision. This technique of the QN spectrum calculation was proposed by Leaver [13].

Now we shall discuss the units of measurements and ranges of the black hole parameters. In this paper we shall measure all the quantities in units of the event horizon. For this we choose the black hole mass, so that $\Delta_r(1) = 0$. Then one has

$$2M = \left(1 - \frac{\Lambda}{3}\right)(1 + a^2) + Q^2.$$

We parametrize the cosmological constant Λ by the parameter $\rho < 1$

$$\Delta_r(1/\rho) = 0 \quad \longrightarrow \quad \frac{\Lambda}{3} = \rho^2 \frac{1 - \rho(a^2 + Q^2)}{1 + \rho + \rho^2(a^2 + Q^2)}.$$

In these units the condition $\Delta_r'(1) > 0$ gives us the range of values of the black hole charge,

$$Q^2 < \frac{1 + 2\rho}{1 + 2\rho + 3\rho^2 + a^2\rho^2} - a^2.$$

The positivity of the right-hand side of the above equation bounds the possible values of the parameter of rotation a,

$$a^2 < \frac{(1 + \rho)\sqrt{1 + 2\rho + 9\rho^2} - (1 + 2\rho + 3\rho^2)}{2\rho^2} \leq 1.$$

III. RESULTS

The quasinormal frequencies of the Kerr-Newman-de Sitter black holes depend on a number of parameters:

(1) black hole parameters: mass M, charge Q, angular momentum a,
(2) field parameters: field charge q and spin s,
(3) cosmological constant Λ,
(4) numbers of modes in the spectrum: the multipole number ℓ, the azimuthal number m, and the overtone number n.

Therefore, if one wants to represent quasinormal frequencies for all values of the above parameters, one has to show a great amount of table data. We decided to be limited here by *representative* tables or plots, which will show dependence of the quasinormal modes on each of the above parameters. Thus, for example, in Fig. 1, one can see the dependence of the $\mathrm{Re}(\omega)$ and $\mathrm{Im}(\omega)$ on the black holes charge Q for fundamental mode $\ell = n = 0$ of perturbations of the scalar field. The real part of ω monotonically grows with the black hole charge Q and the field charge q (note that q can be both positive and negative). For positive values of q, $\mathrm{Re}(\omega)$ attains some maximum value as a function of Q, at some large value of Q. The imaginary part has more complicated behavior: it monotonically decreases as a function of Q until some near extremal value of the black hole charge, keeping meanwhile monotonic dependence on q. Then the curves with different q intersect, that is, the larger q does not guarantee larger $\mathrm{Im}\omega$. Thus if for not very large Q, the charged field decays quicker than the neutral one, for the near extremal Q, the charged field decays slower than neutral. From Fig. 1 one can see that this happens at $Q \sim 0.8 Q_{\mathrm{extr}}$ in the units of the event horizon, while in "$M = 1$ units" this corresponds to $Q \sim 0.995 Q_{\mathrm{extr}}$. Even though the WKB technique, developed until higher orders [14], reproduces this intersection shown in Fig. 1, it could not be easily trusted in this case because of ω dependency of the effective potential [5]. Therefore, confirmation of the intersection with the help of the convergent and accurate Frobenius method leaves apart possible interpretations of charged quasinormal modes in the context of universality of the critical collapse [7]. Let us note also that the nonmonotonic behavior for some curves for real and imaginary parts of ω, near the extremal values of charge, depends on the value qQ and is not new in fact. When approaching the extremal limit of values of Q closely enough, one has the picture of spiraling of the plot of $\mathrm{Re}(\omega)$-$\mathrm{Im}(\omega)$ [15].

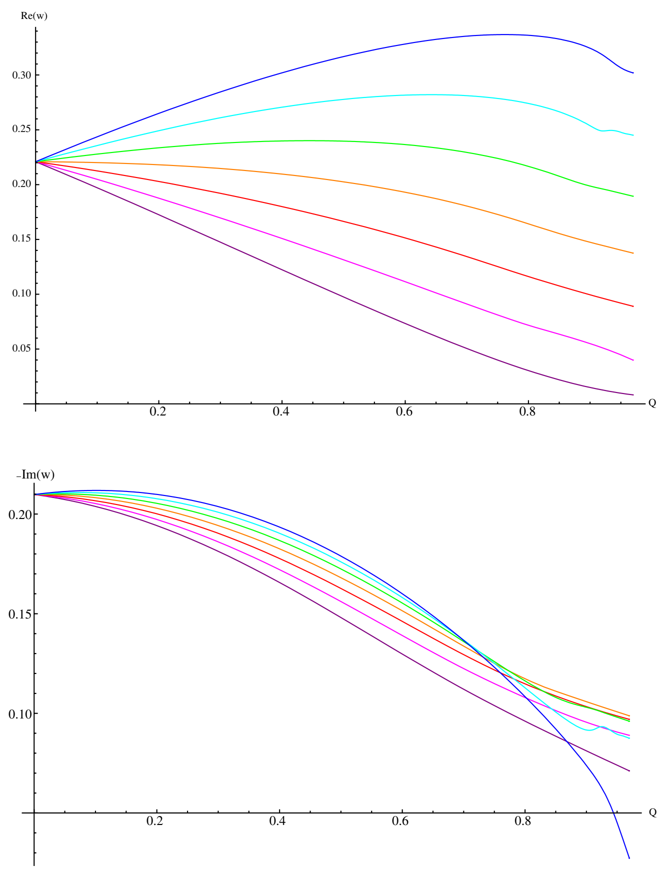

FIG. 1 (color online). Charged (e) scalar field fundamental frequency ($l = 0$) for the Reissner-Nordström black hole as a function of its charge (Q). $q = -0.3$ (purple), $q = -0.2$ (magenta), $q = -0.1$ (red), $q = 0$ (orange), $q = 0.1$ (green), $q = 0.2$ (cyan), $q = 0.3$ (blue). The larger q corresponds to the larger real and larger imaginary (for small black hole charge) part of the QNM.

An important point is the checking of all the known particular limits for our calculations. For $q = Q = 0$ we reproduce the quasinormal modes for the scalar and Dirac fields for Kerr-de Sitter black holes, while for $\Lambda = 0$, $a = 0$ we obtain the limit of pure Reissner-Nordström black holes and the results of [5,6]. For $q = 0$ we find the quasinormal modes for neutral fields for KNdS black holes. When approaching the limit of extreme values of the Λ-term, one can reproduce the exact quasinormal modes obtained as a solution of the Pöschl-Teller equation [16], if $q = a = 0$.

In Fig. 2 we demonstrate the dependence of $\mathrm{Re}(\omega)$ and $\mathrm{Im}(\omega)$ of scalar field modes on the angular momentum a for a few fixed values of the charges Q and q. There one can see that for not large values of qQ, one has the monotonic decay of both real and imaginary parts of ω as a function of a. In other words, the quicker rotating black holes have longer lived modes and smaller real oscillation frequencies. This monotonic behavior breaks for larger values qQ, as it can be seen from the curve $Q = 0.8$, $q = 0.3$ on Fig. 2.

The numerical data for QNMs are represented in Tables I, II, III, and IV and in Figs. 1–3. In Tables I and III, the quasinormal frequencies for different values of multipolar ℓ and azimuthal m numbers are given for the first mode $n = 0$, for some values of the charges Q and q, and for a fixed value of the angular momentum. In Tables II and IV, on the contrary, we fix the values of the black holes charge Q, and consider different values of a and q. From the above table one can see that larger values of the multipole number ℓ, under the same value m, imply larger

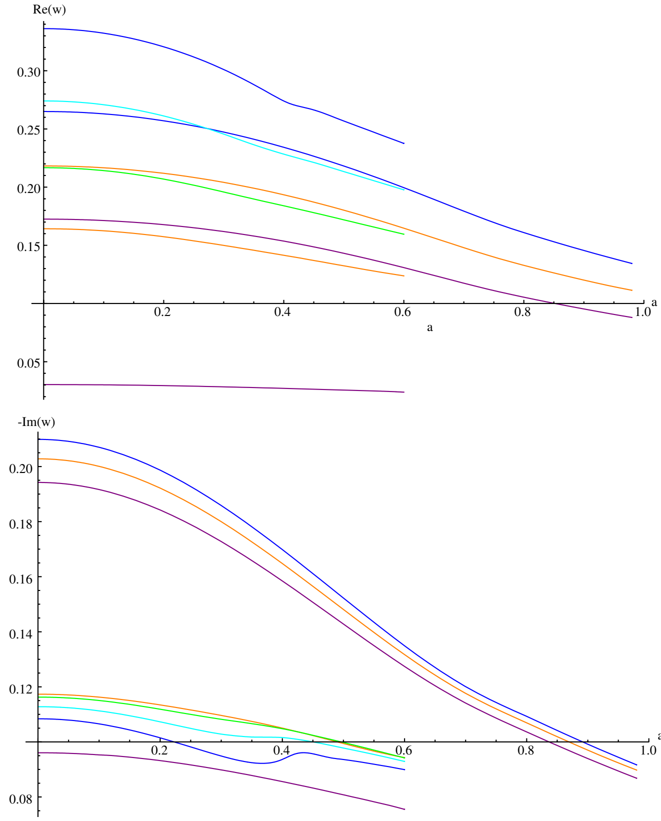

FIG. 2 (color online). Charged (e) scalar field fundamental frequency ($l = 0$) for the Kerr-Newman black hole of charge $Q = 0.2$ ($a < 2\sqrt{6}/5$) and $Q = 0.8$ ($a < 0.6$) as a function of a. $q = -0.3$, $e = 0$ (orange), $q = 0.1$ (green), $q = 0.2$ (cyan), $q = 0.3$ (blue). The larger q corresponds to the larger real and larger imaginary (for small black hole charge) part of the QNM.

TABLE I. QNMs of the scalar perturbation of the Kerr-Newman black holes ($a = 0.4$).

ℓ	m	$Q = 0.2$, $q = -0.3$	$Q = 0.2$, $q = 0$	$Q = 0.2$, $q = 0.3$	$Q = 0.8$, $q = -0.3$	$Q = 0.8$, $q = 0$	$Q = 0.8$, $q = 0.3$
0	0	$0.153\,622 - 0.158\,460i$	$0.193\,444 - 0.164\,777i$	$0.234\,254 - 0.169\,836i$	$0.027\,107 - 0.085\,597i$	$0.141\,475 - 0.105\,014i$	$0.274\,019 - 0.093\,648i$
1	−1	$0.396\,131 - 0.156\,125i$	$0.428\,770 - 0.160\,382i$	$0.462\,269 - 0.164\,345i$	$0.236\,903 - 0.098\,374i$	$0.337\,666 - 0.109\,255i$	$0.452\,137 - 0.115\,708i$
1	0	$0.479\,121 - 0.151\,767i$	$0.514\,846 - 0.154\,723i$	$0.551\,295 - 0.157\,438i$	$0.285\,439 - 0.093\,609i$	$0.399\,817 - 0.098\,162i$	$0.528\,744 - 0.097\,728i$
1	1	$0.603\,295 - 0.145\,951i$	$0.642\,846 - 0.147\,968i$	$0.682\,964 - 0.149\,826i$	$0.364\,922 - 0.075\,864i$	$0.505\,807 - 0.068\,374i$	$0.667\,302 - 0.058\,104i$
2	−2	$0.656\,529 - 0.156\,419i$	$0.688\,008 - 0.159\,179i$	$0.720\,043 - 0.161\,832i$	$0.443\,727 - 0.102\,703i$	$0.543\,278 - 0.109\,491i$	$0.651\,446 - 0.114\,676i$
2	−1	$0.726\,943 - 0.154\,996i$	$0.760\,246 - 0.157\,287i$	$0.794\,064 - 0.159\,477i$	$0.488\,765 - 0.100\,428i$	$0.595\,790 - 0.105\,290i$	$0.711\,645 - 0.108\,424i$
2	0	$0.815\,194 - 0.152\,025i$	$0.850\,587 - 0.153\,847i$	$0.886\,446 - 0.155\,578i$	$0.546\,533 - 0.095\,406i$	$0.663\,393 - 0.097\,610i$	$0.789\,555 - 0.097\,946i$
2	1	$0.927\,889 - 0.147\,965i$	$0.965\,608 - 0.149\,382i$	$1.003\,731 - 0.150\,726i$	$0.625\,000 - 0.085\,165i$	$0.756\,010 - 0.083\,476i$	$0.897\,414 - 0.079\,871i$
2	2	$1.072\,198 - 0.144\,707i$	$1.112\,314 - 0.145\,847i$	$1.152\,765 - 0.146\,933i$	$0.742\,952 - 0.064\,746i$	$0.897\,860 - 0.058\,622i$	$1.064\,754 - 0.052\,886i$

TABLE II. QNMs of the scalar perturbation of the Kerr-Newman black holes ($Q = 0.2$).

ℓ	m	$a = 0.2$, $q = -0.3$	$a = 0.2$, $q = 0$	$a = 0.2$, $q = 0.3$	$a = 0.8$, $q = -0.3$	$a = 0.8$, $q = 0$	$a = 0.8$, $q = 0.3$
0	0	$0.167\,766 - 0.184\,220i$	$0.211\,875 - 0.192\,171i$	$0.257\,011 - 0.198\,680i$	$0.105\,432 - 0.103\,623i$	$0.132\,795 - 0.106\,936i$	$0.160\,904 - 0.109\,273i$
1	−1	$0.470\,255 - 0.176\,446i$	$0.507\,611 - 0.180\,941i$	$0.545\,869 - 0.185\,127i$	$0.266\,598 - 0.109\,174i$	$0.289\,229 - 0.112\,303i$	$0.312\,498 - 0.115\,211i$
1	0	$0.522\,144 - 0.175\,672i$	$0.561\,332 - 0.179\,498i$	$0.601\,338 - 0.183\,046i$	$0.351\,193 - 0.097\,777i$	$0.377\,110 - 0.099\,006i$	$0.403\,534 - 0.100\,059i$
1	1	$0.585\,319 - 0.175\,043i$	$0.626\,523 - 0.178\,296i$	$0.668\,457 - 0.181\,312i$	$0.545\,520 - 0.054\,487i$	$0.578\,091 - 0.054\,264i$	$0.610\,920 - 0.054\,055i$
2	−2	$0.787\,475 - 0.176\,507i$	$0.823\,858 - 0.179\,350i$	$0.860\,824 - 0.182\,078i$	$0.438\,203 - 0.109\,596i$	$0.459\,854 - 0.111\,675i$	$0.481\,918 - 0.113\,676i$
2	−1	$0.834\,779 - 0.176\,198i$	$0.872\,296 - 0.178\,790i$	$0.910\,368 - 0.181\,272i$	$0.505\,143 - 0.106\,753i$	$0.528\,641 - 0.108\,258i$	$0.552\,512 - 0.109\,685i$
2	0	$0.887\,964 - 0.175\,702i$	$0.926\,678 - 0.178\,052i$	$0.965\,915 - 0.180\,299i$	$0.600\,747 - 0.097\,893i$	$0.626\,685 - 0.098\,644i$	$0.652\,951 - 0.099\,329i$
2	1	$0.947\,908 - 0.175\,148i$	$0.987\,872 - 0.177\,273i$	$1.028\,326 - 0.179\,304i$	$0.754\,274 - 0.075\,327i$	$0.783\,768 - 0.075\,164i$	$0.813\,525 - 0.074\,974i$
2	2	$1.015\,500 - 0.174\,741i$	$1.056\,747 - 0.176\,665i$	$1.098\,451 - 0.178\,503i$	$1.039\,415 - 0.048\,194i$	$1.072\,980 - 0.048\,219i$	$1.106\,653 - 0.048\,245i$

TABLE III. QNMs of the Dirac field perturbation of the Kerr-Newman black holes ($a = 0.4$).

ℓ	m	$Q = 0.2$, $q = -0.3$	$Q = 0.2$, $q = 0$	$Q = 0.2$, $q = 0.3$	$Q = 0.8$, $q = -0.3$	$Q = 0.8$, $q = 0$	$Q = 0.8$, $q = 0.3$
1/2	−1/2	0.246 256 − 0.154 133i	0.280 565 − 0.160 311i	0.316 133 − 0.165 779i	0.118 776 − 0.090 357i	0.221 025 − 0.107 204i	0.344 150 − 0.113 238i
1/2	1/2	0.342 822 − 0.141 572i	0.380 628 − 0.144 882i	0.419 348 − 0.147 793i	0.171 964 − 0.078 214i	0.297 229 − 0.073 804i	0.454 538 − 0.058 993i
3/2	−3/2	0.515 027 − 0.155 523i	0.546 793 − 0.158 973i	0.579 262 − 0.162 249i	0.332 623 − 0.100 337i	0.432 175 − 0.108 952i	0.542 690 − 0.114 981i
3/2	−1/2	0.588 694 − 0.153 027i	0.622 736 − 0.155 715i	0.657 409 − 0.158 246i	0.378 403 − 0.097 191i	0.487 664 − 0.102 514i	0.608 266 − 0.105 015i
3/2	1/2	0.687 238 − 0.148 338i	0.723 951 − 0.150 318i	0.761 209 − 0.152 174i	0.442 312 − 0.088 796i	0.565 845 − 0.089 041i	0.701 925 − 0.086 213i
3/2	3/2	0.820 628 − 0.143 438i	0.860 126 − 0.144 895i	0.900 057 − 0.146 265i	0.543 282 − 0.067 958i	0.693 191 − 0.060 714i	0.858 738 − 0.053 488i

TABLE IV. QNMs of the Dirac field perturbation of the Kerr-Newman black holes ($Q = 0.2$).

ℓ	m	$a = 0.2$, $q = -0.3$	$a = 0.2$, $q = 0$	$a = 0.2$, $q = 0.3$	$a = 0.9$, $q = -0.3$	$a = 0.9$, $q = 0$	$a = 0.9$, $q = 0.3$
1/2	−1/2	0.287 309 − 0.174 116i	0.325 875 − 0.180 887i	0.365 774 − 0.186 924i	0.151 829 − 0.097 351i	0.173 649 − 0.101 276i	0.196 306 − 0.104 704i
1/2	1/2	0.340 964 − 0.170 124i	0.381 353 − 0.175 322i	0.422 875 − 0.179 958i	0.260 575 − 0.043 041i	0.289 055 − 0.039 671i	0.318 597 − 0.036 871i
3/2	−3/2	0.615 316 − 0.175 418i	0.651 857 − 0.178 999i	0.689 134 − 0.182 397i	0.311 602 − 0.098 794i	0.331 456 − 0.101 142i	0.351 785 − 0.103 372i
3/2	−1/2	0.663 381 − 0.174 822i	0.701 296 − 0.178 001i	0.739 902 − 0.181 009i	0.378 115 − 0.093 711i	0.400 157 − 0.095 125i	0.422 609 − 0.096 429i
3/2	1/2	0.718 975 − 0.173 997i	0.758 346 − 0.176 798i	0.798 356 − 0.179 445i	0.488 898 − 0.074 552i	0.514 298 − 0.074 568i	0.540 039 − 0.074 515i
3/2	3/2	0.783 304 − 0.173 201i	0.824 167 − 0.175 660i	0.865 612 − 0.177 982i	0.749 656 − 0.064 353i	0.781 326 − 0.064 171i	0.813 053 − 0.064 004i

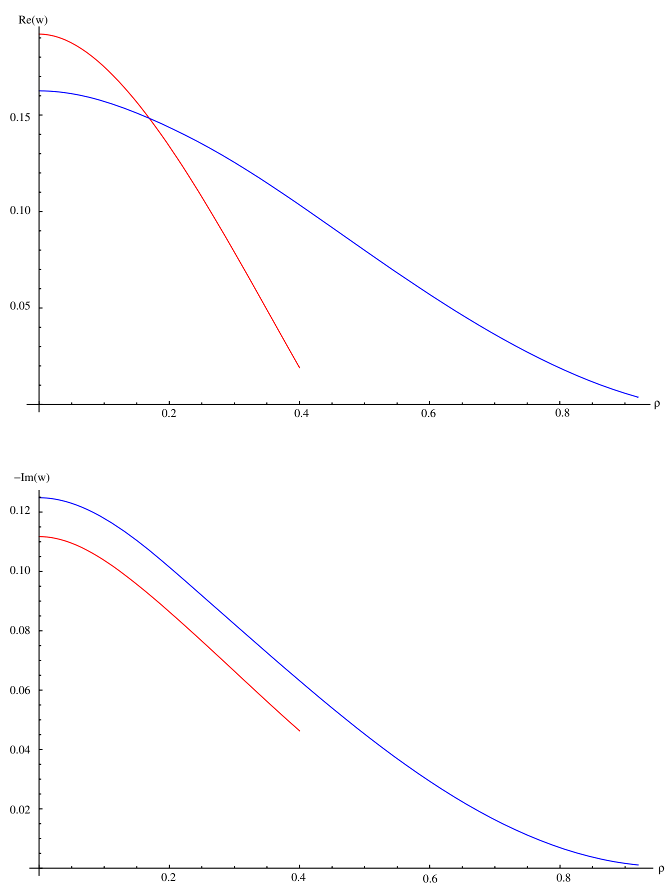

FIG. 3 (color online). Real and imaginary parts of the fundamental QNMs of Kerr-Newman-de Sitter BH $s = l = 1/2$, $m = -1/2$, $Q = 0.2$, $a = 0.8$, $q = 0$ (red) ($\rho < 0.51$) $s = l = m = 0$, $Q = 0.5$, $a = 0.5$, $q = 0$ (blue) ($\rho < 0.94$) as a function of ρ.

Re(ω) and smaller Im(ω). Under some fixed ℓ, large azimuthal numbers give larger Re(ω) and smaller damping rates. When the rotation is large, this decreasing of Im(ω) for larger m is considerable, so that high m modes can be many times longer lived than those for the nonrotating case $a = 0$. This happens for all values of Q and q. Finally, in Fig. 3, one can see the representative dependence of the quasinormal frequencies on the values of the Λ-term. The behavior is qualitatively the same as for the ordinary Schwarzschild-de Sitter black holes [17], that is, the increasing Λ-term suppresses considerably the Reω and Imω, independently on the values of other parameters. Let us note that when all the parameters a, Q, and q are nonvanishing, and the Λ-term approaches near the extremal limit, the Frobenius series converges very slowly, so that we could not reach their extremal limit very closely.

IV. CONCLUSION

In this work, with the help of an accurate convergent Frobenius method, we performed an extensive calculation of quasinormal modes of charged scalar and Dirac fields for Kerr-Newman-de Sitter black holes and have analyzed the dependence of the QN spectrum upon the great variety of parameters of the black holes Q, M, a, of Λ-term, and of the field parameters q and s. This generalizes a number of previous works when only some of the parameters were considered nonvanishing. The model we considered might be successful, when considering the interaction of the charged fields with the electromagnetic background of rotating black holes.

ACKNOWLEDGMENTS

This work was supported by *Fundação de Amparo à Pesquisa do Estado de São Paulo (FAPESP)*, Brazil.

[1] K. D. Kokkotas and B. G. Schmidt, Living Rev. Relativity **2**, 2 (1999).

[2] R. A. Konoplya and A. Zhidenko, Nucl. Phys. **B777**, 182 (2007).

[3] G. T. Horowitz and V. E. Hubeny, Phys. Rev. D **62**, 024027 (2000); D. T. Son and A. O. Starinets, arXiv:0704.0240; A. O. Starinets, Phys. Rev. D **66**, 124013 (2002); V. Cardoso and J. P. S. Lemos, Phys. Rev. D **63**, 124015 (2001); R. A. Konoplya, Phys. Rev. D **68**, 124017 (2003); V. Cardoso, R. Konoplya, and J. P. S. Lemos, Phys. Rev. D **68**, 044024 (2003); G. Michalogiorgakis and S. S. Pufu, J. High Energy Phys. 02 (2007) 023; S. Musiri, S. Ness, and G. Siopsis, Phys. Rev. D **73**, 064001 (2006); I. Amado, C. Hoyos, K. Landsteiner, and S. Montero, arXiv:0706.2750.

[4] H. R. Beyer, Commun. Math. Phys. **221**, 659 (2001); L. E. Simone and C. M. Will, Classical Quantum Gravity **9**, 963 (1992); A. Ohashi and M. a. Sakagami, Classical Quantum Gravity **21**, 3973 (2004); R. A. Konoplya and A. V. Zhidenko, Phys. Lett. B **609**, 377 (2005); R. A. Konoplya and A. Zhidenko, Phys. Rev. D **73**, 124040 (2006); A. Zhidenko, Phys. Rev. D **74**, 064017 (2006); A. Zhidenko, Classical Quantum Gravity **23**, 3155 (2006); E. Berti and K. D. Kokkotas, Phys. Rev. D **67**, 064020 (2003); C. Ma, Y. Gui, W. Wang, and F. Wang, arXiv:gr-qc/0611146; R. Konoplya, Phys. Rev. D **71**, 024038 (2005); R. A. Konoplya and E. Abdalla, Phys. Rev. D **71**, 084015 (2005); R. A. Konoplya and R. D. B. Fontana, arXiv:0707.1156; A. Lopez-Ortega, Gen. Relativ. Gravit. **38**, 1565 (2006).

[5] R. A. Konoplya, Phys. Rev. D **66**, 084007 (2002).

[6] W. Zhou and J. Y. Zhu, Int. J. Mod. Phys. D **13**, 1105 (2004).

[7] R. A. Konoplya, Phys. Lett. B **550**, 117 (2002).

[8] X. He and J. Jing, Nucl. Phys. **B755**, 313 (2006).

[9] J. Jing, Phys. Rev. D **72**, 027501 (2005).

[10] S. Hod and T. Piran, Phys. Rev. D **58**, 024018 (1998); S. Hod and T. Piran, Phys. Rev. D **58**, 024017 (1998);

[11] H. Suzuki, E. Takasugi, and H. Umetsu, Prog. Theor. Phys. **100**, 491 (1998).

[12] A. Zhidenko, Phys. Rev. D **74**, 064017 (2006).

[13] E. W. Leaver, Proc. R. Soc. A **402**, 285 (1985).

[14] B. F. Schutz and C. M. Will, Astrophys. J. Lett. **291**, L33 (1985); S. Iyer and C. M. Will, Phys. Rev. D **35**, 3621 (1987); R. A. Konoplya, J. Phys. Stud. **8**, 93 (2004); Phys. Rev. D **68**, 024018 (2003).

[15] H. Onozawa, T. Mishima, T. Okamura, and H. Ishihara, Phys. Rev. D **53**, 7033 (1996).

[16] V. Cardoso and J. P. S. Lemos, Phys. Rev. D **67**, 084020 (2003).

[17] R. A. Konoplya and A. Zhidenko, J. High Energy Phys. 06 (2004) 037.